



Monitoring the spatial distribution pattern according to urban land use and health risk assessment on potential toxic metal contamination via street dust in Ankara, Türkiye

Oznur Isinkaralar · Kaan Isinkaralar ·
Emine Piriñ Bayraktar

Received: 19 July 2023 / Accepted: 9 August 2023 / Published online: 24 August 2023
© The Author(s), under exclusive licence to Springer Nature Switzerland AG 2023

Abstract The urbanization processes with growing vehicle numbers cause heavy metal pollution in street dust, and high populations in metropolitan cities are exposed to pollutants. This paper aims to monitor the spatial distribution of heavy metals and evaluate the concentrations via health risk assessment of HMs (Cu, Ni, Cd, Co, Pb, and Zn) that expose the inhabitants to health hazards. According to the results of the current study, sixty street dust samples were applied to the acid digestion technique and quantification by inductively coupled plasma-mass spectrometry (ICP-MS). The spatial distribution of the selected heavy metals in the street dust was investigated using the spatial analysis tool in ArcGIS 10.0 according to population density and land use. In the present study, we used hazard index and cancer risk methods to estimate the public health risk of the pollutants exposed to street dust in

Ankara. The concentrations range of the elements in street dust over the study area ranged from 3.34–4.50, 31.69–42.87, 16.09–21.54, 42.85–57.55, 0.00–3.51, and 23.03–30.79, respectively. The overall decreasing order of mean concentration of metals was observed as follows: Pb > Cu > Ni > Co > Cd > Zn. Vehicle traffic and industrial activities seem to be the most critical anthropogenic sources responsible for dust pollution in the study area. The risk assessment of Pb and Ni exposure was the highest, and the hazard index values were 2.42E+00 and 2.28E+00 mg/kg/day for children. However, the effect on adults was 2.62E-01 and 2.37E-02 mg/kg/day, followed by inhalation and dermal contact with street dust was almost negligible. The decreasing concentration is modeled spatially along the western development corridor of the city. The risk to public health is high in areas with high densities close to the city center and the main artery.

O. Isinkaralar (✉)
Department of City and Regional Planning, Faculty
of Engineering and Architecture, 37150 Kastamonu,
Türkiye
e-mail: obulan@kastamonu.edu.tr

K. Isinkaralar
Department of Environmental Engineering, Faculty
of Engineering and Architecture, Kastamonu University,
37150 Kastamonu, Türkiye

E. P. Bayraktar
Department of Elderly Care, Vocational High School
of Health Services, Lokman Hekim University, Ankara,
Türkiye

Keywords Urban air pollution · Urban modelling ·
Health risk assessment · Spatial distribution · Source
apportionment

Introduction

Monitoring urban pollution is a vital research area in detecting existing risks and guiding new planning decisions. Intense consumption, especially in metropolitan cities, has caused pollution to reach levels that threaten public health. Many recent studies have

shown that long-term heavy metal exposure is associated with human health risks and an increased risk of death (Guo et al., 2022; Tägt et al., 2022). Street dust (SD), which allows us to monitor the presence of heavy metals spatially, is solid fine particles containing solid, liquid, and gaseous components and associated air pollutants that seriously threaten human health due to bioaccumulation and urban ecosystems through mobile or stationary sources (Rahman et al., 2019). It is a vital indicator in heavily populated cities significantly affected by intense human activities such as vehicular traffic, industrial emissions, biomass burning, urban construction, and demolition (Wahab et al., 2020). They have increasingly contributed to metal pollution and are enriched in urban areas. For instance, among the basic parameters of urbanization, buildings, constructed buildings, ventilation, and points with interrupted wind flow harm the potential toxic heavy metal (HM) pollution indicators for urban air quality (Al-Shidi et al., 2022). In addition to emissions from various sources, increasing urbanization and motor vehicles have significantly transported and accumulated toxic and harmful pollutants in the SD through atmospheric deposition (Davis & Birch, 2011; Huang et al., 2014).

The increasing absolute concentrations of HMs that have been continuously deposited in the particulate matter have led to public health concerns in densely populated cities due to their nonbiodegradable and persist in the natural environment (Dytlow & Górka-Kostrubiec, 2021). Moreover, SD moves actively in the multiphase regime of the surrounding environment, from airborne redistribution due to intensive human activities to atmospheric deposition (Tang et al., 2013). Numerous recent studies suggest that toxic metal contamination in SD is generally higher than that in soil by widespread human intervention (Chenery et al., 2020; Delibašić et al., 2020; Shahab et al., 2020). The resulting movements cause accumulation and subsequent pollution in various ecosystem chains. With the advancement of the acceleration of industrialization and urbanization, the people who live near city streets that SD reaches indoors through air movement; it can penetrate the human body by respiration, digestion, and skin absorption and consequently becoming detrimental to the health of the inhabitants of the region (Dong et al., 2021a, b; Su et al., 2022). The HMs with strong capacities to migrate, enrich, and contaminate positively correlate

with carcinogenic, teratogenic, and mutagenic effects (Li et al., 2023). Critically, SD has nickel (Ni) and chromium (Cr) from the corrosion of cars, copper (Cu), lead (Pb), zinc (Zn), and cadmium (Cd) from the corrosion of tires and engine parts (Kończak et al., 2021; Miller et al., 2020). Furthermore, all these HMs harm children and adults, depending on their accumulation level. They cause diseases of the nervous, respiratory, and reproductive systems, skin and muscle diseases, and decreased cognitive activity (Kumar et al., 2018; Rehman et al., 2018).

Like other developing countries, Ankara, the capital of Türkiye, is the country's political, economic, administrative, and cultural center. The city has achieved rapid development in the fields of urbanization, industrialization, growing population, limiting natural resources, associated housing, and motorized vehicles, which significantly negatively strained the public urban environment. Evaluation of spatial distribution and associated health risks of HMs in SD has been linked to anthropogenic sources, such as industrial facilities, manufacturing sites, substructure, and street tools, which are still unknown in Ankara city. The accumulation of SD on busy streets, intersection streets of regions, and areas with heavy traffic have shed light on several studies, and the diversity and concentration of HMs have been analyzed for possible pollution effects on urban and human health (Urrutia-Goyes et al., 2018). Reducing the number of vehicles and fossil fuel consumption is one of the primary campaigns that local authorities, environmental organizations, and volunteers are undertaking to help reduce urban pollution to improve public health (Danish et al., 2020; Zhao et al., 2021). Recent studies have focused on exposure to SD pollution and detecting pollution at the intersections of busy streets (Kamani et al., 2018; Pan et al., 2017). These studies examined the size and frequency of streets, the number of vehicles, traffic lights, and their distances to residences to define metal content. In particular, large squares and intersections were found to have higher concentrations and types of HMs in dust than in other areas, probably due to higher traffic density and congestion. Due to the speed of traffic flow on the city's main streets and the absence of traffic lights, toxic metal levels in SD were relatively small, resulting in a low potential impact on human health (Cowan

et al., 2021; Ren et al., 2021). Although different methods were used for sample collection in SD, sweeping was the most common method.

Understanding the toxic metals of SD is essential for controlling atmospheric pollution and growing appropriate pollution mitigation strategies. This work aims to investigate HMs in selected streets of Ankara city and health risk assessment of some selected toxic metals in SD by employing the US-Environmental Protection Agency (US-EPA) health risk estimation model. To the best of our knowledge, this research can serve as a multidisciplinary example of the sources and given the dramatic effects of toxic metals pollution in highly populated traffic roadways, peripheral zones, and industrialized cities across the globe. Supporting, modeling, and evaluating urban spatial research with spatial measurements have become possible by developing geographic information system technology (Dong et al., 2021a, b; Luminati et al., 2021; Yuan et al., 2023). This study analyzed measurements spatially and statistically, based on samples of varying densities and associated with different land use typologies along western development

corridor of Ankara. In addition, it offers an integrated approach that evaluates different population groups based on indexes.

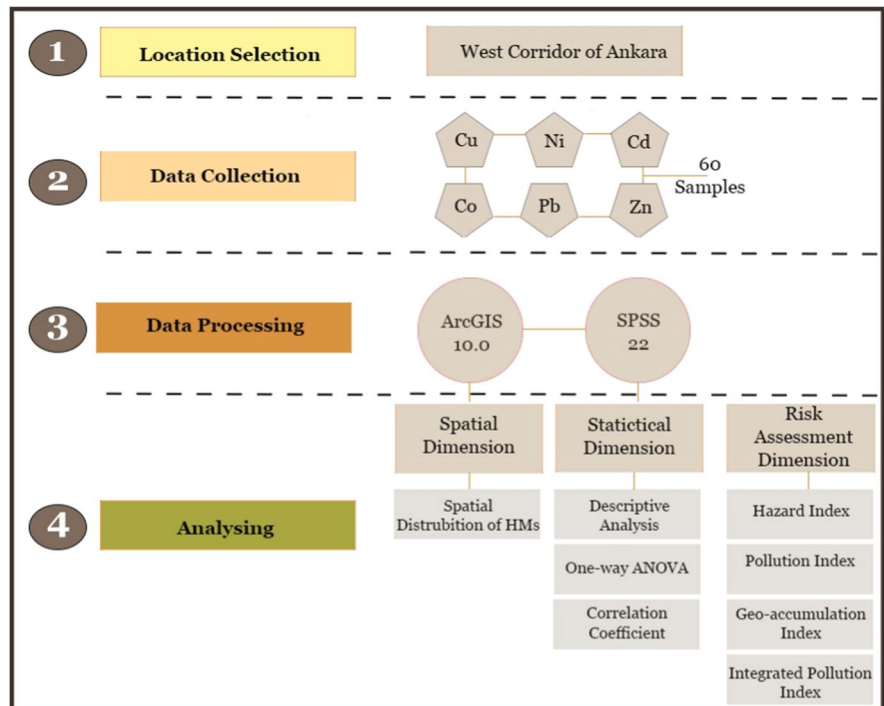
Materials and methods

The data production process of this study consists of four primary stages. These steps are presented in Fig. 1. In the research conducted in Ankara’s Western development corridor, data on six different heavy metals were collected and evaluated in terms of spatial, statistical, and risk assessment dimensions.

Study area

The research site in the following regions is between 39.93170°N and 32.86369°D in Ankara city in Fig. 2. It is the capital of Türkiye, with a rapidly growing population of over 6 million, and is bordered by the eastern and northern highway routes. It is located at an approximate altitude of 890 m from the sea surface. Ankara’s street network covers more than 679 km and is home to more than 1.8 million vehicles circulating

Fig. 1 Flowchart of the study



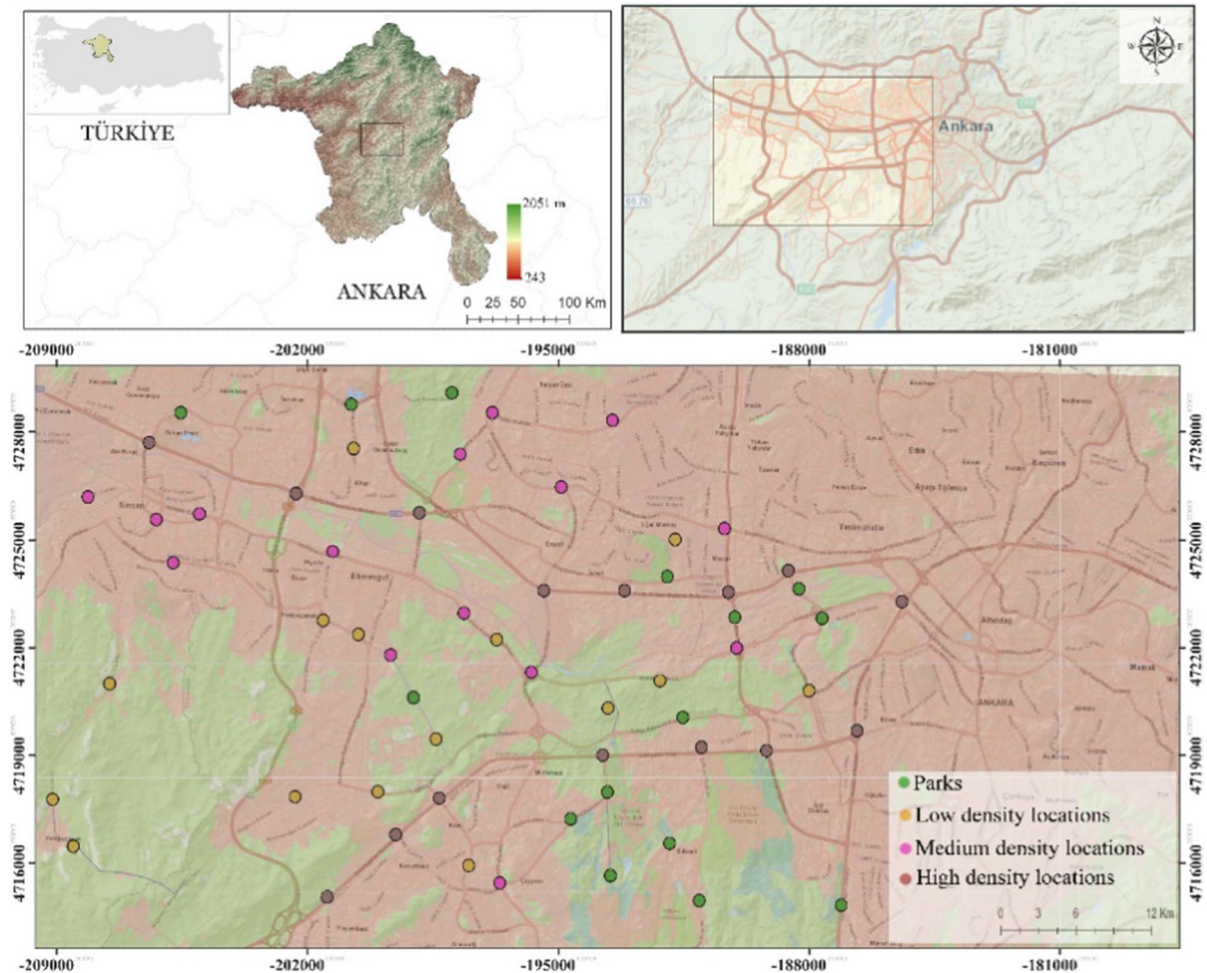


Fig. 2 Geographical position maps of the sampling fields in the Ankara urban area

daily. Although there are minor differences in Ankara's climate, winters in Ankara are freezing, and summers are hot. The yearly average temperature varies from 40 to -24.9 °C. The average annual rainfall varies from approximately 300 to 540 mm, and the humidity in the air varies from 40 to 79%. The temperature difference between day and night is high. Observing the content and spatial distribution of HMs in SD can also provide vital data on the severity of pollution in the surrounding city and the possible associated risks of health effects.

Sampling strategy

In the study area, 60 SD samples taken from twenty key sampling sites were collected from the busiest main street intersections in Ankara city. These intersections

are often referred to as squares. Plastic brushes and sweepers were used for dust collection from streets, sidewalks, and gutters in circles with a 1 ± 0.1 m² radius around each sampling spot for three consecutive days. The brushes were cleaned three times with distilled water before samples were collected. Approximately 200 g of SD composition sampling was placed in sealed polyethylene bags at the operation area, and labeled and then transported to the respective laboratory during September 2022. In addition, all bowls, buckets, and bags used in the study were sterilized.

Laboratory analysis

The homogeneously distributed samples were collected and coded carefully, and brought to the

laboratory for processing. The SD was processed without any contamination, respectively, as follows: (i) samples were dried at 70°C for 96 h, (ii) ground in a mill, (iii) It was sieved through a 100 µm nylon sieve, and (iv) They were stored at 4°C until the methods of digestion. To specify, Cd, Cu, Co, Pb, Zn, and Ni concentrations were digested by microwave-assisted aqua regia digestion. 0.25 g of accurately weighed SD samples in polytetrafluoroethylene-tetrafluoromethane (PTFE-TFM) cups, to which HCl and HNO₃ were added with a 6 and 2 mL ratio. The microwave oven was started for 15 min, and then, the cooling samples were filtered with ultrapure water. The digested container samples were individually analyzed with inductively coupled plasma optical emission spectrometry (ICP-OES).

Data analysis

Each SD sample was taken in replicate, and reproducibility was ensured by the paired Student’s *t*-test at a 95% confidence level. Descriptive statistics were outlined values of minimum, maximum, mean, and standard deviations (SD), coefficients of variation (CV) using the IBM Statistical Product and Service Solution (SPSS) Statistics 22 software. Followed by a box plot outlining the data scatter (25th quartiles, the median, the mean, and the 75th percentiles), Pearson correlation analysis for the relationship between metals, and principal component analysis (PCA) for quantitative resource allocation were employed to assess HM variables in SD.

Risk assessment model

Exposure dose

People are directly or indirectly subjected to SD by ingestion, inhalation, and dermal contact. The intake rates and particle emissions that form the basis for non-carcinogenic and cumulative carcinogenic risks were calculated for Cd, Cu, Co, Pb, Zn, and Ni for three exposure pathways in Ankara. Various HMs in SD were also evaluated to quantify the carcinogenic–non-carcinogenic hazards for both adults and children. Therefore, the equations are used in the United States Environmental Protection Agency’s

methodology for measuring exposure to HMs in SD (US EPA, 1986, 1989, 1993, 1996). The formulas by the Exposure Factors Handbook (US EPA, 1997) were also used to depict the average daily dose (ADD) (mg/kg/day) of Cd, Cu, Co, Pb, Zn, and Ni via ADD_{ing} (through ingestion), ADD_{inh} (via inhalation), ADD_{dermal} (via dermal contact), ADD_{vapor} (via vapor), and average daily dose over a lifetime (LADD).

$$ADD_{ing} = C \times \frac{IngR \times EF \times ED}{BW \times AT} \times 10^{-6} \tag{1}$$

$$ADD_{inh} = C \times \frac{InhR \times EF \times ED}{PEF \times BW \times AT} \tag{2}$$

$$ADD_{dermal} = C \times \frac{SL \times SA \times ABS \times EF \times ED}{BW \times AT} \times 10^{-6} \tag{3}$$

$$ADD_{vapor} = C \times \frac{InhR \times EF \times ED}{VF \times BW \times AT} \tag{4}$$

$$LADD = \frac{C \times EF}{PEF \times AT} \times \left(\frac{InhR_{child} \times ED_{child}}{BW_{child}} + \frac{InhR_{adult} \times ED_{adult}}{BW_{adult}} \right) \tag{5}$$

where *C* is related to the concentration of HMs (mg/kg); the exposure factors for adults and children in IngR (ingestion rate) were 100 and 200 mg/d, and InhR (inhalation rate) were 20 and 7.6 m³/day. EF is exposure frequency within 180 day/year for children, and ED is exposure duration between 6 and 24 years for children and adults. BW is the average body weight accepted as 15 and 70 for children and adults; AT is the average exposure time (ED×365) and 25,550 for non-carcinogenic and carcinogenic children. Particle emission factor (PEF) is 1.36×10⁹ m³/kg in children, the skin adherence factor (SL) is 0.2 and 0.07 mg/cm²/day, and the exposed area of the skin (SA) is 2800 and 5700 cm² for children and adults. Also, the dermal absorption factor (ABS) is 0.001 as unitless.

Furthermore, hazard indexes (HI) and hazard quotient (HQ) were calculated for carcinogenic–non-carcinogenic impacts for each pathway of exposure in the present analysis. When the HI value is ≤ 1, it indicates that no relevant non-carcinogenic adverse effect risks have been identified. What if HI > 1 means that non-carcinogenic effects can occur; the more HI goes up, the more likely the event will occur (US EPA, 2001).

$$HQ_{ing} = \frac{ADD_{ing} \times RBA}{RfD_{ing}}$$

$$HQ_{inh} = \frac{ADD_{inh}}{RfD_{inh}}$$

$$HQ_{dermal} = \frac{ADD_{dermal}}{RfD_{dermal}}$$

$$HQ_{vapor} = \frac{ADD_{vapor}}{RfD_{vapor}} HI \sum_1^i HQ$$

$$PI = \frac{C_n}{B_n} \tag{7}$$

$$I_{geo} = \log_2 \left(\frac{C_n}{1.5B_n} \right) \tag{8}$$

Pollution and geo-accumulation index

To determine soil quality, a pollution index (PI) and an integrated pollution index (IPI) for Cd, Cu, Co, Pb, Zn, and Ni were calculated using the concentrations and background values in Eq. (7). IPI is derived from the mean value of PI for each metal. PI and IPI indicate pollutants grade as follows: low ($IPI \leq 1$), moderate ($1 < IPI \leq 2$), and high ($IPI > 3.0$). The geo-accumulation index (I_{geo}) has been described to show metal contamination levels in SD by the geological and anthropogenic origins of the trace elements in Eq. (8) (Müller, 1969). C_n is the total concentration of these metals, and B_n is the background concentration of the metals concerning PI and I_{geo} . The I_{geo} is classified into seven groups to increase one by one from uncontaminated (< 0) to highly contaminated (> 5).

Results and discussion

Spatial distribution pattern of HMs

Studying the spatial distribution of HMs in urban road dust is helpful for detecting areas of hotspots with high concentrations of HMs and assessing potential sources. Consideration should be given to multiple anthropogenic factors in using geostatistical techniques in the urban environment. Spatial distribution maps of HMs in the study area were prepared using ordinary Kriging interpolation with ArcGIS 10.0. SD spatial distribution of Cd, Cu, Co, Pb, Zn, and Ni can reflect possible HM sources in Fig. 3. The distribution patterns of the six elements commonly controlled by human activities share the same features. Some prominent intense polluted hotspots are usually located at higher levels in the southern and western parts of the study area. This trend is probably related to the local prevailing wind direction (northeast wind). Among these elements, lead shows a more diffuse distribution

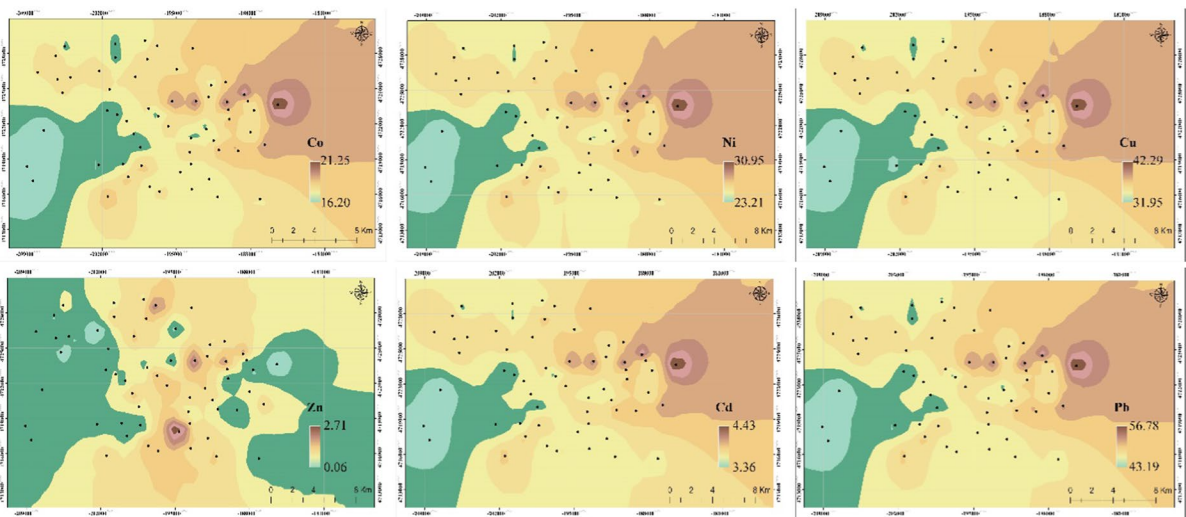


Fig. 3 Spatial distribution of HM concentrations in SD

and prominent Pb pollution hotspots are in the city’s center. Therefore, Pb is still the most abundant pollutant in the SD of Ankara and should have priority in pollution control.

Relative to the other cities inside and outside the countries, the HM concentration of HMs was lower than that in many territories, except Pb, Cd, and Ni. Moving to more urbanized zones may contribute to an overall increase in the prevalence of HM in such places (Istanbullu et al., 2023). Kabir et al. (2022) investigated various toxic HMs for contamination and spatial distribution in Kushtia, Bangladesh. Industrial emissions, agricultural applications, and heavy traffic activities have released Pb, Cu, Cr, Zn, Ni, and As with dust samples in this region. The spatial distribution maps have occurred for a more contaminated site named St-5, derived from pollution due to the central point of transportation and other anthropogenic activities.

Similarly, Bisht et al. (2022) reported that the spatial distribution of Zn, Cu, Ni, and Pb in the several zones of Dehradun city was related to fossil fuel burning and vehicle parts abrasion. Fan et al. (2022) demonstrated PTMs contamination in resuspended SD, leading to ecological–health risks in the Shijiazhuang. Thus this research was to estimate overall contamination assessment and spatial distribution maps of potentially toxic metals. Their regular and non-normal distributions were considered in terms of similar spatial distribution tendencies. They show dominant sources of metals in urban regions. Cd, Cu, Ni, and Zn can come from petroleum combustion, while Pb and Cr are multiple sources from the combustion of coal fossil fuels. Cd, Cr, and Ni have also

followed a relatively diffuse spatial distribution pattern in particular areas, whereas Cd has a comparatively dispersed spatial distribution. Relatively higher Cd and Zn contents were detected in the hotspots of industrial areas and cultivated land at the confluence point (Men et al., 2018). Wu et al. (2022) identified sources of heavy metal pollution, respectively, heavy industry, improper agricultural practices, and urban development in China. In a study conducted in the Lintong District of Shaanxi Province, a characteristic arid zone in northwestern China, farming sources 65.5% of heavy metals.

In comparison, traffic was 17.9%, and natural factors 11.1% (Liu et al., 2023). While Bisht et al., (2022) identified the pollutant heavy metal pollution as vehicle-derived in their analysis in India, Skorbiłowicz et al. (2023) statistically modeled high Cr, Cu, Ni, Zn, and Pb concentrations in locations with high traffic flow, the presence of shopping malls, administrative buildings, and bus stations. In the case of Ankara, the impact of urban activities and vehicular circulation is monitored spatially.

Amount of HM content in SD

Statistical descriptions of the selected toxic metals in the research region are listed, and the results of ‘one-way ANOVA are in Table 1. The mean Cd, Cu, Co, Pb, Zn, and Ni concentrations in Ankara SD were mg/kg, respectively. The concentrations range of Cd, Cu, Co, Pb, Zn, and Ni in SD over the study area ranged from 3.34–4.50, 31.69–42.87, 16.09–21.54, 42.85–57.55, 0.00–3.51, and 23.03–30.79

Table 1 Statistical descriptive data and one-way ANOVA analysis of HM concentrations (mg/kg)

		Co	Ni	Cu	Zn	Cd	Pb	
	Minimum	16.09	23.03	31.69	0.00	3.34	42.85	
	Maximum	21.54	30.79	42.87	3.51	4.50	57.55	
	Mean	17.99	25.86	35.66	0.88	3.75	48.07	
	Median	17.88	25.66	35.36	0.76	3.72	47.71	
	SD	1.16	1.61	2.32	0.65	0.23	3.02	
	CV	0.70	0.60	0.50	0.14	0.68	0.72	
	Kurtosis	0.89	0.96	1.09	3.17	1.21	0.98	
	Skewness	0.91	0.87	0.95	1.38	0.93	0.93	
	F	2.580	2.594	0.566	5.098	0.536	6.021	
SD Standard Deviation, CV Coefficient of Variation	Mean Square	Between groups	1.300	2.496	5.185	1.885	0.051	8.874
		Within groups	2.240	4.201	9.154	3.154	0.096	14.295
Significant at 0.001 level	Significance	0.041*	0.028*	0.836	0.000	0.854	0.000***	

respectively. The overall decreasing order of mean concentration of metals was observed to be as shown below: $Pb > Cu > Ni > Co > Cd > Zn$. The maximum Cd, Cu, Co, Pb, Zn, and Ni concentrations in the SD are 4.5, 42.87, 21.54, 57.55, 3.51, and 30.79 mg/kg. In relative terms, Pb and Ni are the most significant contributor to HM contamination via traffic density and population. However, the average amount of Zn was smaller than other metals. Pb and Zn values are significant at 0.001 level.

Other metals except Zn determined high coefficients of variation (CV: 0.5–0.72) that their combination sources probably affected high inhomogeneity in SD. Moderate coefficients of variation for Zn (0.14) reflect a relatively normal distribution. The skewness values of metals except Zn fall outside between -1 and $+1$. Also, Kurtosis represented the extent of outliers without Zn, indicating the non-normal distribution by human activities.

Figure 4 illustrates a box plot of the HM concentrations (mg/kg) in SD at the 25th and the 75th percentiles, with the solid black line in the box representing the 50th percentile along with the error bars. It displays the min–max values of metal samples in SD.

The uppermost and lowest horizontal lines indicate the maximum and minimum values.

Many studies have been conducted on SD in several cities, finding a positive correlation between burning fossil fuels, industrial activities, and toxic metal accumulation (Habibi et al., 2022; Sobhanardakani, 2019). Kamani et al. (2017) inferred that SD has HM content and spatial/temporal distributions of Cd, Cr, Cu, Ni, Pb, and Zn performed in Tehran, Iran. They reported that pollutants' mean concentrations varied in the order of $Zn > Cu > Pb > Ni > Cr > Cd$ by anthropogenic causes such as urban transportation and traffic activities. Abbasi et al. (2017) revealed the two primary sources: (i) Cu, Zn, Sb, Hg, Pb, and Mo from road traffic emissions and (ii) Al, Mn, Ni, Ti, Cd, and Co from suspended soil particles. Due to oil refineries and heavy traffic load in Bushehr City, they detected higher concentrations of HMs in SD than in world soils. Alsbou and Al-Khashman (2018) measured Cd, Cu, Fe, Pb, and Zn concentrations in the SD of Petra, Jordan. This study concluded that anthropogenic activities primarily contribute to toxic metal pollution. Similar research for SD in Shijiazhuang by Cai and Li (2019) proved that Cd, Cr, Cu, Hg, Ni, Pb,

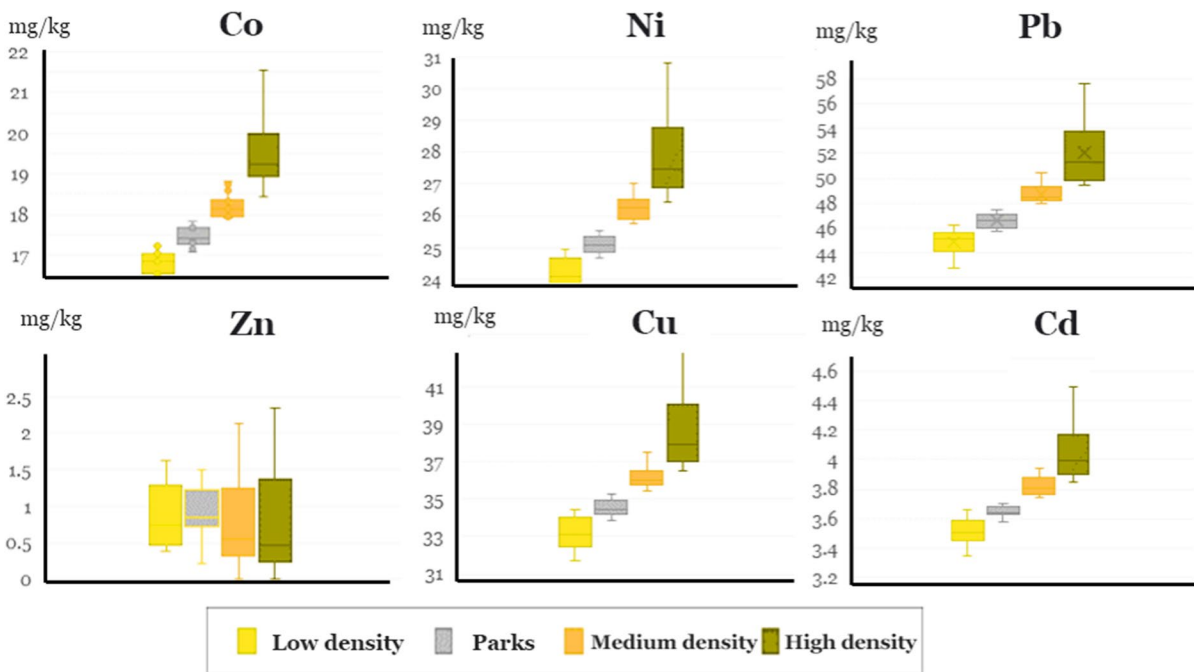


Fig. 4 Box plots showing frequency changes of toxic metal concentrations in SD

and Zn concentration was evaluated as notably higher (5 and 917 times) from human sources.

We have compared the HM composition of SD, Cd, Cu, Co, Pb, Zn, and Ni concentrations in Ankara are relatively high compared to the population, industry, and traffic pattern. The outcome of research studies has demonstrated that Cd, Pb, Cu, and Ni are most directly related to anthropogenic sources and the possibility of adverse health effects due to exposure to spatial variation in urban environments.

Correlation coefficient analysis

Pearson’s correlation analysis was executed for hot points to establish the inter-metal relationships in the road dust samples in Table 2. Co shows a strong positive correlation with Ni, Cu, Cd, and Pb where $r=0.997, 0.995, 0.994,$ and 0.995 . A statistically significant and positive correlation was observed for Ni and Cu ($r=0.996$), Cd ($r=0.996$), and Pb (0.995), which may indicate similar sources, such as vehicular emission. Cd and Pb are strongly correlated with each other.

Principle Component Analysis (PCA)

Table 3 shows the factor loading, eigenvalues of the factors, and percentage variances in PCA analysis. The analysis results present 99.788% of the total variance, and first component (PC1), first component (PC2), and first component (PC3) accounted for 82.97, 16.70, and 11.11% of the variance.

Table 4 shows PI values of toxic metals in SD. The min and max values of PI for Cd, Co, Cu, Ni, Pb, and Zn were 25.42–34.60, 2.30–3.08, 1.06–1.43, 1.54–2.05, 2.86–3.84, and 0.01–0.04. Cd and Pb exhibited higher IPI values with 28.90 and

Table 3 PCA loadings of essential principal components variables

Parameters	Component		
	PC1	PC2	PC3
Cd	0.997	0.017	0.060
Co	0.998	0.018	−0.001
Cu	0.997	0.038	−0.040
Ni	0.998	0.024	0.018
Pb	0.998	−0.005	−0.034
Zn	0.018	1.000	0.000
Eigenvalue	4.891	1.999	0.907
% of variance	82.97	16.70	11.11
Cumulative %	82.97	99.67	99.78

Extraction and rotation method present principal component analysis and varimax with Kaiser normalization

3.21; 51.7 and 48.3% of SD samples depicted high pollution levels. Also, Co was moderate level pollution with 2.57 for IPI in 45% of SD samples. Cu and Ni values indicate middle-level pollution, although Zn had the lowest contamination.

Table 5 presents the I_{geo} values determined that Cd was more significant than 0 for all SD samples and ranged from 4.10 to 4.53. These values suggested heavy to highly contaminated, and Pb values indicate between 0.93 and 1.35 for moderately contaminated with anthropogenic sources. Ni had an I_{geo} of 0.03–0.45, with 53.3% of SD samples having an I_{geo} greater than 0 (uncontaminated to moderately contaminated). Cu and Zn I_{geo} values less than 0 were classified as not contaminated with Cu and Zn.

Human health risk assessment of HMs

Table 6 displays the carcinogens and non-carcinogen effects of Cd, Co, Cu, Ni, Pb, and Zn (mg/kg/

Table 2 Pearson’s correlations matrix for the metal concentrations

	Co	Ni	Cu	Zn	Cd	Pb
Co	1					
Ni	0.997**	1				
Cu	0.995**	0.996**	1			
Zn	0.036	0.042	0.056	1		
Cd	0.994**	0.996**	0.994**	0.035	1	
Pb	0.995**	0.995**	0.994**	0.013	0.994**	1

**Correlation is significant at the 0.01 level (2-tailed)

Table 4 Pollution index (PI) and an integrated pollution index (IPI) of HMs

Elements	Pollution index (PI)			NOE*	ROE** (%)	Contamination level
	Min	Max	Mean (IPI)			
Cd	25.72	34.60	28.90	31	51.7	High
Co	2.30	3.08	2.57	27	45	Moderate
Cu	1.06	1.43	1.19	29	48.3	Middle
Ni	1.54	2.05	1.72	30	50	Middle
Pb	2.86	3.84	3.21	29	48.3	High
Zn	0.01	0.04	0.01	52	86.7	Low

*NOE The number of individual metal-containing dust samples that exceed the classification values.

**ROE Percentage to exceed classification ratings

Table 5 I_{geo} values of HMs

Elements	I_{geo}			NOE*	ROE** (%)	Anthropogenic influences
	Min	Max	Mean			
Cd	4.10	4.53	4.27	29	48.3	Heavily to extremely contaminated
Co	0.62	1.04	0.77	31	51.7	Uncontaminated to moderately contaminated
Cu	-0.51	-0.07	-0.34	38	63.3	Uncontaminated
Ni	0.03	0.45	0.20	32	53.3	Uncontaminated to moderately contaminated
Pb	0.93	1.35	1.09	9	15	Moderately contaminated
Zn	-8.76	-4.68	-6.90	54	90	Uncontaminated

Table 6 Exposure risks of cancer and non-cancer of toxic metals

	Elements	Children				Adult			
		HQ _{ing}	HQ _{inh}	HQ _{dermal}	HI	HQ _{ing}	HQ _{inh}	HQ _{dermal}	HI
Non-carcinogenic	Cu	3.14E-01	2.0363E-07	5.56E-05	3.15E-01	3.37E-02	7.64784E-08	8.49E-05	3.38E-02
	Co	4.92E-01	1.32E-06	5.14E-02	5.44E-01	5.53E-02	1.32E-06	5.14E-02	1.07E-01
	Cd	5.75E-03	7.89E-07	6.46E-03	1.22E-02	6.16E-04	7.89E-07	1.07E-02	1.14E-02
	Pb	2.42E+00	2.89E-06	1.58E-03	2.42E+00	2.59E-01	2.89E-06	2.61E-03	2.62E-01
	Ni	2.28E+00	2.87E-07	8.96E-05	2.28E+00	2.37E-02	1.08E-07	1.47E-05	2.37E-02
	Zn	3.09E-01	9.71E-09	3.03E-06	3.09E-01	3.21E-03	3.65E-09	4.96E-07	3.21E-03
For carcinogens	Cu	1.96E-02	2.0363E-07	5.56E-05	1.96E-02	8.39E-03	7.64784E-08	8.49E-05	8.47E-03
	Co	3.06E-02	1.43302E-06	5.59E-02	8.66E-02	1.38E-02	1.43302E-06	5.59E-02	6.97E-02
	Cd	3.58E-04	8.58807E-07	7.03E-03	7.39E-03	1.53E-04	8.58807E-07	1.07E-02	1.09E-02
	Pb	1.51E-01	3.13333E-06	1.71E-03	1.52E-01	6.45E-02	3.13333E-06	2.61E-03	6.71E-02
	Ni	1.42E-01	2.86808E-07	8.96E-05	1.42E-01	5.91E-03	1.07718E-07	1.47E-05	5.92E-03
	Zn	1.92E-02	9.71304E-09	3.03E-06	1.92E-02	8.00E-04	3.64799E-09	4.96E-07	8.01E-04

day) in SD for children and adults. Upon comparing, the assessment results of Pb and Ni exposure were the highest, and HI values were 2.42E+00 and 2.28E+00 mg/kg/day for children; however, Pb and Ni effects to adults were 2.62E-01 and 2.37E-02 mg/kg/day. Exposure levels via ingestion ranged from 10^{-4} to 10^0 in all SD, while the inhalation and dermal contact exposure were 10^{-9} to 10^{-2} , about 10^{-5} to 10^{-2}

times lower than ingestion. Ingestion via the mouths of SD samples is a more prominent contributor to health risks for children and could be ignored compared with the risk from inhalation and dermal contact. The exposure risk of Cu (8.47E-03 mg/kg/day) and Zn (8.01E-04 mg/kg/day) for carcinogenic risk was low and acceptable in adults.

Relevant for both children and adults, other researchers have also noted parallel trends between atmospheric dust and human exposure (Hosseini et al., 2020; Sobhanardakani, 2018). Wang et al. (2020) explored potential toxic metal pollution and its non-carcinogenic and carcinogenic health risks for children and adults. The hazard index and carcinogenic risk index were determined as health risk indicators. The mean HQs for children were 9, 6.6, and 1.8 times the values of adults for ingestion, dermal contact, and inhalation. Jiang et al. (2018) calculated health risks using HQ, HI, and CR from exposure to multiple metals in Lanzhou. For human carcinogens, HI values for children were 0.249 for Cr, and no non-carcinogenic risks for adults were 2.32×10^{-2} below the safe level. Trojanowska and Świetlik (2019) assessed health risks with traffic-related Cr, Cu, Fe, Mn, Ni, Pb, and Zn in the SD of Radom, Poland. They were used to estimate human health risks through direct ingestion, inhalation, and dermal absorption, the main pathway for children and adults.

Conclusion

Dust pollution significantly threatens urban air quality, leading to public health issues. This study investigated the contamination state, primary sources, chemical speciation, and health risk assessment of 6 metals in SD of Ankara. The concentrations, risk status, and current levels of the HMs studied in this research were compared with other cities in the relevant literature. The results show that SD in Ankara has high metal concentrations. Cd, Pb, and Ni are derived mainly from street transportation sources; Cu and Co have a natural and anthropogenic mixed source; Zn is derived from local soil. The sequence of mobilization order based on the sum of the sequential extraction steps of the modified BCR is $Pb > Cu > Ni > Co > Cd > Zn$. Pb and Ni posed higher risk factors for children, and exposure levels by ingestion ranged from 10^{-4} to 100 for all SDs, while inhalation and dermal contact exposure ranged from 10^{-9} to 10^{-2} , which is approximately 10^{-5} to 10^{-2} times lower than ingestion. While compared to adults, children were more sensitive to exposure to non-carcinogenic and carcinogenic risks compared to adults. It indicates that Ankara's ambient urban quality is relatively poor, and traffic emissions are the dominant source of

pollution on the main roads. Furthermore, the tracking should be strengthened to preserve the health of the inhabitants. Toxic metal species in resuspended SD affect its environmental behavior and risks and should be studied in the future. The current distribution reflects the risk of heavy metal accumulation in the central and roadside parcels that constitute the city's more pitted topography. The spatial distribution pattern extending from the city center to the west corridor critically analyzes discussions about falling concentrations at the peripheries and compact and sprawling city models.

Author contribution Ozgur Isinkaralar: conceptualization, software, writing original draft, processing analysis, interpretation, formal analysis. Kaan Isinkaralar: conceptualization, software, writing original draft, processing analysis, interpretation, formal analysis, review and editing. Emine Piriç Bayraktar: processing analysis, interpretation, data curation, software, formal analysis, review and editing.

Data availability The data that support the findings of this study are available from the corresponding author, upon reasonable request.

Declarations

Ethics approval Not applicable.

Consent to participate Not applicable.

Consent for publication Not applicable.

Competing interests The authors declare no competing interests.

References

- Abbasi, S., Keshavarzi, B., Moore, F., Delshab, H., Soltani, N., & Sorooshian, A. (2017). Investigation of microrubbers, microplastics and heavy metals in street dust: A study in Bushehr city. *Iran. Environmental Earth Sciences*, 76, 1–19. <https://doi.org/10.1007/s12665-017-7137-0>
- Alsoub, E. M. E., & Al-Khashman, O. A. (2018). Heavy metal concentrations in roadside soil and street dust from Petra region, Jordan. *Environmental Monitoring and Assessment*, 190, 1–13. <https://doi.org/10.1007/s10661-017-6409-1>
- Al-Shidi, H. K., Al-Reasi, H. A., & Sulaiman, H. (2022). Heavy metals levels in road dust from Muscat, Oman: Relationship with traffic volumes, and ecological and health risk assessments. *International Journal of*

- Environmental Health Research*, 32(2), 264–276. <https://doi.org/10.1080/09603123.2020.1751806>
- Bisht, L., Gupta, V., Singh, A., Gautam, A. S., & Gautam, S. (2022). Heavy metal concentration and its distribution analysis in urban road dust: A case study from most populated city of Indian state of Uttarakhand. *Spatial and Spatio-temporal Epidemiology*, 40, 100470. <https://doi.org/10.1016/j.sste.2021.100470>
- Cai, K., & Li, C. (2019). Street dust heavy metal pollution source apportionment and sustainable management in a typical city—Shijiazhuang, China. *International Journal of Environmental Research and Public Health*, 16(14), 2625. <https://doi.org/10.3390/ijerph16142625>
- Cheney, S. R., Sarkar, S. K., Chatterjee, M., Marriott, A. L., & Watts, M. J. (2020). Heavy metals in urban road dusts from Kolkata and Bengaluru, India: Implications for human health. *Environmental Geochemistry and Health*, 42, 2627–2643. <https://doi.org/10.1007/s10653-019-00467-4>
- Cowan, N., Blair, D., Malcolm, H., & Graham, M. (2021). A survey of heavy metal contents of rural and urban roadside dusts: Comparisons at low, medium and high traffic sites in Central Scotland. *Environmental Science and Pollution Research*, 28, 7365–7378. <https://doi.org/10.1007/s11356-020-11081-8>
- Danish, Z., & J., Hassan, S. T., & Iqbal, K. (2020). Toward achieving environmental sustainability target in organization for economic cooperation and development countries: The role of real income, research and development, and transport infrastructure. *Sustainable Development*, 28(1), 83–90. <https://doi.org/10.1002/sd.1973>
- Davis, B. S., & Birch, G. F. (2011). Spatial distribution of bulk atmospheric deposition of heavy metals in metropolitan Sydney, Australia. *Water, Air, & Soil Pollution*, 214, 147–162. <https://doi.org/10.1007/s11270-010-0411-3>
- Delibašić, Š., Đokić-Kahvedžić, N., Karić, M., Keskin, I., Velispahić, A., Huremović, J., ... & Pašalić, A. (2020). Health risk assessment of heavy metal contamination in street dust of federation of Bosnia and Herzegovina. *Human and Ecological Risk Assessment: An International Journal*, 27(5), 1296–1308. <https://doi.org/10.1080/10807039.2020.1826290>
- Dong, H., Xue, M., Xiao, Y., & Liu, Y. (2021a). Do carbon emissions impact the health of residents? Considering China's industrialization and urbanization. *Science of the total environment*, 758, 143688. <https://doi.org/10.1016/j.scitotenv.2020.143688>
- Dong, J., Ma, R., Cai, P., Liu, P., Yue, H., Zhang, X., ... & Song, X. (2021b). Effect of sample number and location on accuracy of land use regression model in NO₂ prediction. *Atmospheric Environment*, 246, 118057. <https://doi.org/10.1016/j.atmosenv.2020.118057>
- Dytłow, S., & Górka-Kostrubiec, B. (2021). Concentration of heavy metals in street dust: An implication of using different geochemical background data in estimating the level of heavy metal pollution. *Environmental Geochemistry and Health*, 43, 521–535. <https://doi.org/10.1007/s10653-020-00726-9>
- Fan, P., Lu, X., Yu, B., Fan, X., Wang, L., Lei, K., ... & Rinklebe, J. (2022). Spatial distribution, risk estimation and source apportionment of potentially toxic metal (loid) s in resuspended megacity street dust. *Environment International*, 160, 107073. <https://doi.org/10.1016/j.envint.2021.107073>
- Guo, X., Su, W., Li, N., Song, Q., Wang, H., Liang, Q., ... & Sun, C. (2022). Association of urinary or blood heavy metals and mortality from all causes, cardiovascular disease, and cancer in the general population: A systematic review and meta-analysis of cohort studies. *Environmental Science and Pollution Research*, 29(45), 67483–67503. <https://doi.org/10.1007/s11356-022-22353-w>
- Habibi, H., Sobhanardakani, S., Cheraghi, M., Lorestani, B., & Sadr, M. K. (2022). Analysis, sources and health risk assessment of trace elements in street dust collected from the city of Hamedan, west of Iran. *Arabian Journal of Geosciences*, 15(2), 168. <https://doi.org/10.1007/s12517-022-09460-1>
- Hosseini, N. S., Sobhanardakani, S., Cheraghi, M., Lorestani, B., & Merrikhpour, H. (2020). Heavy metal concentrations in roadside plants (*Achillea wilhelmsii* and *Cardaria draba*) and soils along some highways in Hamedan, west of Iran. *Environmental Science and Pollution Research*, 27, 13301–13314. <https://doi.org/10.1007/s11356-020-07874-6>
- Huang, W., Duan, D., Zhang, Y., Cheng, H., & Ran, Y. (2014). Heavy metals in particulate and colloidal matter from atmospheric deposition of urban Guangzhou. *South China. Marine Pollution Bulletin*, 85(2), 720–726. <https://doi.org/10.1016/j.marpolbul.2013.12.041>
- Istanbulu, S. N., Sevik, H., Isinkaralar, K., & Isinkaralar, O. (2023). Spatial distribution of heavy metal contamination in road dust samples from an urban environment in Samsun, Türkiye. *Bulletin of Environmental Contamination and Toxicology*, 110(4), 78. <https://doi.org/10.1007/s00128-023-03720-w>
- Jiang, Y., Shi, L., Guang, A. L., Mu, Z., Zhan, H., & Wu, Y. (2018). Contamination levels and human health risk assessment of toxic heavy metals in street dust in an industrial city in Northwest China. *Environmental Geochemistry and Health*, 40, 2007–2020. <https://doi.org/10.1007/s10653-017-0028-1>
- Kabir, M. H., Kormoker, T., Shammi, R. S., Tusher, T. R., Islam, M. S., Khan, R., ... & Idris, A. M. (2022). A comprehensive assessment of heavy metal contamination in road dusts along a hectic national highway of Bangladesh: Spatial distribution, sources of contamination, ecological and human health risks. *Toxin Reviews*, 41(3), 860–879. <https://doi.org/10.1080/15569543.2021.1952436>
- Kamani, H., Mahvi, A. H., Seyedsalehi, M., Jaafari, J., Hoseini, M., Safari, G. H., ... & Ashrafi, S. D. (2017). Contamination and ecological risk assessment of heavy metals in street dust of Tehran, Iran. *International journal of environmental science and technology*, 14, 2675–2682. <https://doi.org/10.1007/s13762-017-1327-x>
- Kamani, H., Mirzaei, N., Ghaderpoori, M., Bazrafshan, E., Rezaei, S., & Mahvi, A. H. (2018). Concentration and ecological risk of heavy metal in street dusts of Eslamshahr. *Iran. Human and Ecological Risk Assessment: An International Journal*, 24(4), 961–970. <https://doi.org/10.1080/10807039.2017.1403282>
- Kończak, B., Cempa, M., & Deska, M. (2021). Assessment of the ability of roadside vegetation to remove particulate matter from the urban air. *Environmental Pollution*, 268, 115465. <https://doi.org/10.1016/j.envpol.2020.115465>

- Kumar, A., Singh, N., Pandey, R., Gupta, V. K., & Sharma, B. (2018). Biochemical and molecular targets of heavy metals and their actions. Biomedical applications of metals, 297–319. https://doi.org/10.1007/978-3-319-74814-6_14
- Li, Y., Ye, Z., Yu, Y., Li, Y., Jiang, J., Wang, L., ... & Liu, M. (2023). A combined method for human health risk area identification of heavy metals in urban environments. *Journal of Hazardous Materials*, 449, 131067. <https://doi.org/10.1016/j.jhazmat.2023.131067>
- Liu, J., Kang, H., Tao, W., Li, H., He, D., Ma, L., ... & Li, X. (2023). A spatial distribution–Principal component analysis (SD-PCA) model to assess pollution of heavy metals in soil. *Science of The Total Environment*, 859, 160112. <https://doi.org/10.1016/j.scitotenv.2022.160112>
- Luminati, O., de Campos, B. L. D. A., Flückiger, B., Brentani, A., Rösli, M., Fink, G., & de Hoogh, K. (2021). Land use regression modelling of NO₂ in São Paulo, Brazil. *Environmental Pollution*, 289, 117832. <https://doi.org/10.1016/j.envpol.2021.117832>
- Men, C., Liu, R., Xu, F., Wang, Q., Guo, L., & Shen, Z. (2018). Pollution characteristics, risk assessment, and source apportionment of heavy metals in road dust in Beijing, China. *Science of the Total Environment*, 612, 138–147. <https://doi.org/10.1016/j.scitotenv.2017.08.123>
- Miller, D. J., Actkinson, B., Padilla, L., Griffin, R. J., Moore, K., Lewis, P. G. T., ... & Alvarez, R. A. (2020). Characterizing elevated urban air pollutant spatial patterns with mobile monitoring in Houston, Texas. *Environmental Science & Technology*, 54(4), 2133–2142. <https://doi.org/10.1021/acs.est.9b05523>
- Müller, G. (1969). Index of geoaccumulation in sediments of the Rhine River. *GeoJournal*, 2, 108–118.
- Pan, H., Lu, X., & Lei, K. (2017). A comprehensive analysis of heavy metals in urban road dust of Xi’an, China: Contamination, source apportionment and spatial distribution. *Science of the Total Environment*, 609, 1361–1369. <https://doi.org/10.1016/j.scitotenv.2017.08.004>
- Rahman, M. S., Khan, M. D. H., Jolly, Y. N., Kabir, J., Akter, S., & Salam, A. (2019). Assessing risk to human health for heavy metal contamination through street dust in the Southeast Asian Megacity: Dhaka, Bangladesh. *Science of the Total Environment*, 660, 1610–1622. <https://doi.org/10.1016/j.scitotenv.2018.12.425>
- Rehman, K., Fatima, F., Waheed, I., & Akash, M. S. H. (2018). Prevalence of exposure of heavy metals and their impact on health consequences. *Journal of Cellular Biochemistry*, 119(1), 157–184. <https://doi.org/10.1002/jcb.26234>
- Ren, Y., Luo, Q., Zhuo, S., Hu, Y., Shen, G., Cheng, H., & Tao, S. (2021). Bioaccessibility and public health risk of heavy Metal (loid) s in the airborne particulate matter of four cities in northern China. *Chemosphere*, 277, 130312. <https://doi.org/10.1016/j.chemosphere.2021.130312>
- Shahab, A., Zhang, H., Ullah, H., Rashid, A., Rad, S., Li, J., & Xiao, H. (2020). Pollution characteristics and toxicity of potentially toxic elements in road dust of a tourist city, Guilin, China: Ecological and health risk assessment. *Environmental Pollution*, 266, 115419. <https://doi.org/10.1016/j.envpol.2020.115419>
- Skorbiłowicz, M., Trybułowski, Ł., & Skorbiłowicz, E. (2023). Spatial distribution and pollution level of heavy metals in street dust of the city of Suwałki (Poland). *International Journal of Environmental Research and Public Health*, 20(6), 4687. <https://doi.org/10.3390/ijerph20064687>
- Sobhanardakani, S. (2018). Human health risk assessment of potentially toxic heavy metals in the atmospheric dust of city of Hamedan, west of Iran. *Environmental Science and Pollution Research*, 25(28), 28086–28093. <https://doi.org/10.1007/s11356-018-2818-0>
- Sobhanardakani, S. (2019). Ecological and human health risk assessment of heavy metal content of atmospheric dry deposition, a case study: Kermanshah. *Iran. Biological Trace Element Research*, 187, 602–610. <https://doi.org/10.1007/s12011-018-1383-1>
- Su, M., Wang, Q., Li, R., & Wang, L. (2022). Per capita renewable energy consumption in 116 countries: The effects of urbanization, industrialization, GDP, aging, and trade openness. *Energy*, 254, 124289. <https://doi.org/10.1016/j.energy.2022.124289>
- Tägt, J., Helte, E., Donat-Vargas, C., Larsson, S. C., Michaëlsson, K., Wolk, A., ... & Åkesson, A. (2022). Long-term cadmium exposure and fractures, cardiovascular disease, and mortality in a prospective cohort of women. *Environment International*, 161, 107114. <https://doi.org/10.1016/j.envint.2022.107114>
- Tang, R., Ma, K., Zhang, Y., & Mao, Q. (2013). The spatial characteristics and pollution levels of metals in urban street dust of Beijing, China. *Applied Geochemistry*, 35, 88–98. <https://doi.org/10.1016/j.apgeochem.2013.03.016>
- Trojanowska, M., & Świetlik, R. (2020). Investigations of the chemical distribution of heavy metals in street dust and its impact on risk assessment for human health, case study of Radom (Poland). *Human and Ecological Risk Assessment: An International Journal*, 26(7), 1907–1926. <https://doi.org/10.1080/10807039.2019.1619070>
- Urrutia-Goyes, R., Hernandez, N., Carrillo-Gamboa, O., Nigam, K. D. P., & Ornelas-Soto, N. (2018). Street dust from a heavily-populated and industrialized city: Evaluation of spatial distribution, origins, pollution, ecological risks and human health repercussions. *Ecotoxicology and Environmental Safety*, 159, 198–204. <https://doi.org/10.1016/j.ecoenv.2018.04.054>
- US EPA. (United States Environmental Protection Agency) (1986). Superfund Public Health Evaluation Manual. EPA/540/1–86.
- US EPA. (1989). Risk assessment guidance for superfund, Vol. I: Human Health Evaluation Manual.
- US EPA. (1993). Reference dose (RfD): description and use in health risk assessments. Background Document 1A. Integrated risk information system (IRIS).
- US EPA. (1996). Soil screening guidance: Technical background document. EPA/540/R-95/128. Office of Solid Waste and Emergency Response.
- US EPA. (1997). Exposure factors handbook. EPA/600/P-95/002F. Washington, DC, EPA, Office of Research and Development.
- US EPA. (2001). Supplemental guidance for developing soil screening levels for superfund sites. OSWER 9355.4–24 Office of Solid Waste and Emergency Response.
- Wahab, M. I. A., Abd Razak, W. M. A., Sahani, M., & Khan, M. F. (2020). Characteristics and health effect of heavy metals on non-exhaust road dusts in Kuala Lumpur. *Science of the Total Environment*, 703, 135535. <https://doi.org/10.1016/j.scitotenv.2019.135535>

- Wang, X., Liu, E., Lin, Q., Liu, L., Yuan, H., & Li, Z. (2020). Occurrence, sources and health risks of toxic metal (loid)s in road dust from a mega city (Nanjing) in China. *Environmental Pollution*, 263, 114518. <https://doi.org/10.1016/j.envpol.2020.114518>
- Wu, Y., Li, X., Yu, L., Wang, T., Wang, J., & Liu, T. (2022). Review of soil heavy metal pollution in China: Spatial distribution, primary sources, and remediation alternatives. *Resources, Conservation and Recycling*, 181, 106261. <https://doi.org/10.1016/j.resconrec.2022.106261>
- Yuan, X., An, T., Hu, B., & Zhou, J. (2023). Analysis of spatial distribution characteristics and main influencing factors of heavy metals in road dust of Tianjin based on land use regression models. *Environmental Science and Pollution Research*, 30(1), 837–848. <https://doi.org/10.1007/s11356-022-22151-4>
- Zhao, J., Xi, X. I., Na, Q. I., Wang, S., Kadry, S. N., & Kumar, P. M. (2021). The technological innovation of hybrid and plug-in electric vehicles for environment carbon pollution control. *Environmental Impact Assessment Review*, 86, 106506. <https://doi.org/10.1016/j.eiar.2020.106506>

Publisher's Note Springer Nature remains neutral with regard to jurisdictional claims in published maps and institutional affiliations.

Springer Nature or its licensor (e.g. a society or other partner) holds exclusive rights to this article under a publishing agreement with the author(s) or other rightsholder(s); author self-archiving of the accepted manuscript version of this article is solely governed by the terms of such publishing agreement and applicable law.